Radionuclide calibrator responses for ^{224}Ra in solution and adsorbed on calcium carbonate microparticles

Elisa Napoli,[1,2,3,4] Jeffrey T. Cessna,[1] Leticia Pibida,[1] Ryan Fitzgerald,[1] Gro E. Hjellum,[2] and Denis E. Bergeron[1]*

[1]Physical Measurement Laboratory, National Institute of Standards and Technology, Gaithersburg, MD 20899-8462, USA
[2]Oncoinvent AS, Oslo, Norway
[3]Institute of Clinical Medicine, University of Oslo, Oslo, Norway
[4]Department of Radiation Biology, Institute for Cancer Research, Oslo University Hospital, Oslo, Norway.

*denis.bergeron@nist.gov

Abstract

A suspension of ^{224}Ra adsorbed onto $CaCO_3$ microparticles shows promise for α-therapy of intracavitary micro-metastatic diseases. To facilitate accurate activity administrations, geometry-specific calibration factors for commercially available reentrant ionization chambers (ICs) have been developed for $^{224}RaCl_2$ solutions and ^{224}Ra adsorbed onto $CaCO_3$ microparticles in suspension in ampoules, vials, and syringes. Ampoules and vials give IC responses consistent with each other to < 1%. Microparticles attenuation leads to a ≈ 1% to ≈ 2.5% reduction in response in the geometries studied.

Key Words: Ionization chamber; dose-response relationship; alpha therapy; geometry; attenuation

1. Introduction

Radium-224, with its emission of alpha particles from its decay and its clinically appealing half-life ($T_{1/2}$ = 3.631(2) d) (Bé et al., 2004), has historically been considered for radiotherapeutic applications (Pappenheim and Plesch, 1912). The electronic configuration of radium resembles that of calcium, thus when injected into the body, radium is conveyed to the bones and is often referred to as a "bone-seeker" (US National Research Council 1988; Juzeniene et al., 2018). This property leads radium to target osteoblastic bone metastases (Sartor et al., 2013). The bone-seeking property of radium as ^{224}Ra was exploited medically over many years (1950-2005) (Koch et al., 1978; Kommission Pharmakotherapie, 2001; Wick and Gössner, 1993; Eckert & Ziegler, 2019), although not in cancer therapy but as palliative treatment for ankylosing spondylitis disease. Nowadays, another α-emitting radium isotope, ^{223}Ra-dichloride (Xofigo, Bayer)[†], is used for treatment of patients with skeletal metastases from castration-resistant prostate cancer (Kluetz et al., 2014). Internal beta-emitting radiation therapy with radiolabeled particles has been a treatment option for cancers with intracavitary dissemination (Rosenshein et al., 1979). Recently, a suspension of injectable calcium carbonate microparticles ($CaCO_3$) labeled with the alpha-emitter ^{224}Ra has shown promise in preclinical studies for treatment of cavitary micro-metastatic cancer (Westrøm et al., 2018, 2018b).

The National Institute of Standards and Technology (NIST) developed a primary standard for ^{224}Ra activity based on triple-to-double coincidence ratio (TDCR) liquid scintillation (LS) counting measurements and confirmed by CIEMAT-NIST efficiency tracing (CNET) with

[†] Certain commercial equipment, instruments, or materials are identified in this paper to foster understanding. Such identification does not imply recommendation by the National Institute of Standards and Technology, nor does it imply that the materials or equipment identified are necessarily the best available for the purpose.

tritium and live-timed 4παβ(LS)-γ(NaI) anticoincidence (LTAC) counting (Napoli et al., 2020). In clinical applications, activity measurements are achieved with commercially available reentrant ionization chambers (IC) commonly referred to as radionuclide calibrators or "dose calibrators". Accurate assays require appropriate formulation- and geometry-specific calibration factors, or "dial settings" (*DS*s). Dial settings for ^{224}Ra have been evaluated by Napoli (Napoli et al., 2020) for 5 mL of a 1 mol/L HCl solution of ^{224}Ra in secular equilibrium with its progeny, in a NIST standard 5 mL flame-sealed ampoule, for several Capintec (Florham Park, New Jersey, USA) radionuclide calibrators using the calibration curve method (Zimmerman and Cessna, 2001).

The purpose of this study is to assess user-friendly coefficients that permit an IC reading response translation based on solution composition, volume, and container used to avoid possible bias in the activity determination. Because of the relatively low energy x-rays and bremsstrahlung encountered in the beta decay of some daughters of ^{224}Ra, changes in sample composition may affect the results of measurements with ionization chambers (Zimmerman and Cessna, 2001; Zimmerman et al.,2001; Calhoun et al., 1987). The characteristics of the container and the chemical composition of the sample will affect attenuation, so this study determines accurate geometry-specific *DS*s for ^{224}Ra in solution and adsorbed onto $CaCO_3$ microparticles. Dial settings and correction factors are reported for labeled microparticles in vials and syringes. While these may not ultimately represent the composition or shipping/administration container of a clinical or commercial product (clinical sites should always calibrate administered activities according to the manufacturer's instructions), the results reported here give a general sense of the direction and magnitude of ^{224}Ra assay biases wrought by changes in composition and container.

2. Material and Methods

All solutions, chemicals, and equipment used in the particle labeling process were provided by Oncoinvent AS, Norway. The calcium carbonate microparticles were produced by Oncoinvent AS, Norway as described for the second generation microparticles by Westrøm *et al*. (Westrøm et al., 2018). The concentration of particles in suspension used for all experiments was 250 mg/mL and the activity range for the samples was 1 MBq to 2 MBq. A total of three experiments (identified as E4, E5, and E6), each using a separate shipment of ^{224}Ra solution (0.5 mL of $^{224}RaCl_2$ in 1 mol/L HCl in a v-vial) from Oak Ridge National Laboratory (ORNL), were performed to establish calibrations for (and determine corrections for) different measurement geometries with potential clinical relevance. E4 was dedicated to establishing dose calibrator settings for 20 mL dose vials (20R adaptiQ, ready to use EBB vials # 1557349, Schott USA) containing different volumes (from 2 mL to 20 mL) of $^{224}RaCl_2$ in 1 mol/L HCl or water; comparing these measurements should reveal any difference in attenuation among different solutions and volume amounts. In E4, the activity concentration of the master solution was determined by triple-to-double coincidence ratio (TDCR) liquid scintillation counting, as described in the development of ^{224}Ra primary standard by Napoli *et al*. (2020). E5 established attenuation factors by comparing dose calibrator measurements on 20 mL dose vials containing 20 mL of $^{224}RaCl_2$ in 1 mol/L HCl and vials containing ^{224}Ra radiolabeled $CaCO_3$ microparticles in suspension. The microparticles were suspended in “water for injection” (WFI), which is high quality sterile water without significant chemical impurities and particularly suitable for injection. Finally, in E6, 20 mL syringes (Luer lock tip 20 mL SOFT-JECT syringe, purchased form Henke-Sass Wolf GmbH (HSW), Germany) containing either aqueous ^{224}Ra or labeled microparticles in suspension, were used. Before filling, the syringe tips were sealed with epoxy

to prevent spillage. Plungers were added to seal the filled syringe sources with the aid of small-gauge tungsten wire, cut to be inserted into the barrel of the syringe, terminating just above the liquid level. The wire breaks the seal of the plunger against the syringe wall, allowing the plunger to be carefully depressed into the epoxy-sealed syringe. Instead of needles, luer lock stoppers were affixed to the luer locks for additional safety. The $CaCO_3$ microparticles were suspended and labeled in 12 mL of WFI in the syringes. More details are presented in section 2.1. Attenuation factors were established by comparing measurements of syringes containing microparticles to measurements of syringes containing $^{224}RaCl_2$ only (Figure 1). In E5 and E6, the activity concentration of each master solution was determined by measuring 5 mL ampoules containing $^{224}RaCl_2$ in water or 1 mol/L HCl solution, on ionization chambers (AutoIC) (Fitzgerald, 2010), using the calibration factors determined during the primary standardization (Napoli et al., 2020). A custom-built plexiglass syringe dipper (housing 22 mm Ø, Capintec), suitable for the 20 mL syringe used, was delivered both at NIST and Oncoinvent. The custom dipper is identical to the standard Capintec dipper in all respects except that the bore of the hole in the syringe position is wider to accommodate the larger syringe in the hanging position.

2.1. Source preparation

Dilutions of the ^{224}Ra sources received from ORNL (one for each experiment conducted), were carried out with 1 mol/L HCl. All sources were prepared gravimetrically, using the aspirating pycnometer method (Sibbens and Altzitzoglou, 2007); when practicable, both dispensed and contained masses were measured. To assure neutral pH and protect the $CaCO_3$ microparticles from attack by HCl, an appropriate aliquant of 1 mol/L NaOH was added to each “water” or

microparticle suspension source prior to the addition of ^{224}Ra in HCl. In E5 and E6, $CaCO_3$ microparticles were labeled according to the ^{224}Ra $CaCO_3$ microparticle surface-labeling protocol explained by Westrøm *et al*. (2018). Small adaptations of the original protocol reported by Westrøm *et al*. were made: $CaCO_3$ microparticles (nominal concentration of 250 mg/mL) in suspension with sulfate, barium and saline solutions, were transferred by means of a calibrated micropipette directly into vials or syringes for the incubation step, when ^{224}Ra is added, so that the labeling process was carried out *in situ* without the final wash of the particles mentioned in Westrøm *et al*. (Westrøm et al., 2018). We show in section 3.2 that unbound ^{224}Ra after the incubation step was < 1 %. This differs from the typical procedure wherein microparticles are labeled with ^{224}Ra before being dispensed into vials or syringes. The change was necessary so that the activity of ^{224}Ra in each source was directly linked by mass to calibration sources prepared in each experiment (section 2.2).

2.2. Ionization chamber measurements

In each experiment, ampoules were measured on multiple reentrant ionization chambers (ICs) to calibrate the activity concentration of the master solution later used to calculate the activity dispensed into different sources. The precisely known activities of the various sources enabled us to determine composition- and geometry-specific calibration factors. For all *DS* determinations, the calibration curve method (Zimmerman and Cessna, 2001) was used. For measurements on the Capintec instruments, a LabVIEW-based interface was used to record multiple readings at each *DS*. Sources were also measured on the Vinten 671 ionization chamber (VIC), which is read directly by a Keithley 6517 electrometer, which feeds the measured currents to a PC via a

LabVIEW interface. The VIC at NIST is related to a sister chambers at other laboratories, including the National Physical Laboratory (NPL) in Teddington, UK, allowing for indirect comparison of activity standards (Bergeron and Cessna, 2018). Calibration coefficients for the VIC (K_{VIC}) are expressed directly as a function of current in units of pA/MBq. Monte Carlo simulations of the VIC response were carried out using the EGSnrc DOSRZnrc Rev 1.5.5 code (Rogers et al., 2010) with geometric and materials inputs adapted from Townson *et al*. (2018). The model was validated by reproducing absolute efficiencies reported by Townson *et al*. to 0.2 % for 1000 keV photons and 2.9 % for 30 keV photons, with 0.3 % and 1.3 % statistical uncertainties, respectively.

2.3. Gamma-ray spectrometry measurements

In each experiment, ampoules were measured on high-purity germanium (HPGe) detectors to check for photon-emitting impurities, confirm secular equilibrium, and estimate solution activities based on Decay Data Evaluation Project (DDEP) gamma emission probabilities (Bé et al., 2004). No photon-emitting impurities were detected near the reference time in any of the experiments; typical limits were similar to those reported in Napoli *et al*. (Napoli et al., 2020). At later times, HPGe detected ^{228}Th breakthrough. In every experiment except E6, the activity fraction, $A_{\text{Th-228}}/A_{\text{Ra-224}}$, at the separation time was $< 5\cdot10^{-6}$. In experiment E6, HPGe spectrometry indicated $A_{\text{Th-228}}/A_{\text{Ra-224}} = 9.7\cdot10^{-4}$ at the separation time. ORNL was informed of the unexpectedly high ^{228}Th content, and the anomaly was attributed to the use of a polypropylene column for the separation instead of the glass ion exchange columns used in all the other experiments.

We performed EGSnrc Monte Carlo calculations (model described in Zimmerman et al., 2015) using DDEP photon emission probabilities and nuclide ratios calculated from the Bateman equation to estimate IC responses with different initial ^{228}Th fractions and different measurement times. These suggested that the ^{228}Th impurity in E6 would affect the measured IC responses by < 0.2 %. Therefore, no corrections were made, but a 0.2 % uncertainty component was added. Moreover, the calculations showed that the impurity in E6 results in an expected bias to the apparent half-life (as seen 6 d to 15 d after separation) of < 0.07 %.

3. Results

3.1. Measuring $^{224}RaCl_2$ solutions in 20 mL glass vials (Experiment 4)

In E4, the goals were to establish dose calibrator settings (*DS*s) for dose vials, whether volume corrections will be necessary over the range of 2 mL to 20 mL of solution, and finally, whether measurements in neutral water would differ from measurements in acid due to, e.g., adsorption on container walls or radon gas diffusion.

All data used to calculate *DS*s or correction factors were collected after secular equilibrium had been established (between 2 d and 3 d after source preparation and > 6 d after ^{224}Ra separation from ^{228}Th). An example of an equilibrating source is shown in Figure 2; similar plots were scrutinized in E4 for all sources on all instruments. As in other experiments, the reference time (t_{ref}) was selected to minimize decay-correction uncertainties in the measurements.

Dial setting determinations for one 5mL NIST flame sealed ampoule (A2) and two 20 mL dose vials, one containing 20 mL of acid solution (V1) and one containing 2 mL of acid solution (V7),

are summarized in Table 1. The uncertainties on the dial settings (e.g., Table 2) are mostly due to the standard error on the fit to the calibration curve (0.4 % to 0.6 %) and the uncertainty on the standard activity (≈ 0.3 %).

In addition to geometry-specific *DS* determinations, relative calibrator responses were measured. For the various geometries considered in E4, calibrator responses were measured at a single *DS* and then related in terms of ratios that could be applied as correction factors, *k*, that will allow a user to translate the reading response (*R*) among different containers used: ampoules (a), vials (v), syringes (s) and different solution volume (*V*) and composition: 1 mol/L HCl (A) or water (W).

$$R_{\mathrm{v},V,\mathrm{A}} = R_{\mathrm{a,5,A}} * k_{\mathrm{a,5,A}}^{\mathrm{v},V,\mathrm{A}} \tag{1}$$

$$R_{\mathrm{v},V,\mathrm{W}} = R_{\mathrm{a,5,A}} * k_{\mathrm{a,5,A}}^{\mathrm{v},V,\mathrm{A}} * k_{\mathrm{v},V,\mathrm{A}}^{\mathrm{v},V,\mathrm{W}} \tag{2}$$

where in equation 1, the chamber response at a given dial setting for an ampoule containing 5 mL of acid solution ($R_{\mathrm{a,5,A}}$) is related to the response for a vial containing a given volume, *V*, of acid solution ($R_{\mathrm{v},V,\mathrm{A}}$) by a factor, $k_{\mathrm{a,5,A}}^{\mathrm{v},V,\mathrm{A}}$, which is determined experimentally as the ratio of the two measured responses. Similarly, in equation 2 corrections for sample composition are possible with an additional factor, $k_{\mathrm{v},V,\mathrm{A}}^{\mathrm{v},V,\mathrm{W}}$, which is also determined experimentally.

The series of vials labeled E4-V1 to E4-V7 in E4 revealed a slight volume-dependence in the chamber response (Figure 3), with the largest volumes returning the weakest chamber response. Relative responses were averaged for sources in each geometry and correction factors were calculated according to equations 1 and 2. The results, summarized in Table 3, suggest that the chamber response is lower for the vial containing 20 mL of solution than for the ampoule

containing 5 mL. This could arise due to increased photon attenuation by the thicker vial glass, increased self-absorption due to the larger diameter of the vial, and/or decreased geometric efficiency due to the solution height. Moreover, chamber responses are slightly larger for water samples than acid samples. This is consistent with the greater density of acid solutions, but we cannot rule out increased efficiency in water samples due to adsorption of ^{224}Ra to the vial walls. In addition to the Capintec chambers, sources were measured on the VIC. With its thinner chamber walls, the VIC is more sensitive to the lower-energy photons that are more affected by changes in source geometry. The volume-dependence of the VIC response was more pronounced (Figure 4). Correction factors (Table 4) were calculated as for the Capintec chambers. Monte Carlo simulations gave $k_{\mathrm{v,5,A}}^{\mathrm{v,20,A}}$ = 0.9780 (33) which, as shown in Figure 4, confirms the general trend of experimental data. The results of further Monte Carlo simulations of 5 mL of water at various heights imply that most (about 86 %) of the volume effect is due to changes in attenuation (self-absorption) rather than to height.

For the Capintec chambers, the geometry effects measured in E4 are of similar magnitude to their uncertainties and it appears that dose vials containing $^{224}RaCl_2$ solutions can be measured with the same *DS*s determined for ampoules without introducing significant bias.

3.2. Measuring suspension of labeled microparticles in vials (Experiment 5)

In E5, sources were prepared in 20 mL vials with distilled deionized water and labeled microparticles. The goals were to: label the microparticles *in situ* and determine efficiency of the ^{224}Ra adsorption and retention on the microparticles; determine whether attenuation by the $CaCO_3$ microparticles significantly affects chamber response and establish correction factors, if

necessary; and determine whether particle attenuation is significantly different for suspended versus sedimented microparticles.

The labeling efficiency and labeled particle stability were monitored in the series of 1.5 mL glass v-vials labeled L0, L1, L2 and L3. The supernatant was removed (via a 1 mL syringe) from L1 on Day 1, from L2 on Day5, and from L3 on Day 7. Figure 5 shows ionization chamber responses, normalized to the L0 (control) response, demonstrating that the removal of the supernatant minimally impacts the total activity contained in the vial. The *in situ* procedure appears to yield high labeling efficiency (> 99 %) with no observable desorption.

The different calibrator responses for the various geometries considered in E5 are represented in terms of ratios that could be applied as correction factors. To equations 1 and 2, we add equation 3 to relate the chamber response for a vial containing labeled microparticles ($R_{\mathrm{v},V,\mathrm{P}}$) to the response expected for a vial containing water:

$$R_{\mathrm{v},V,\mathrm{P}} = R_{\mathrm{v},V,\mathrm{W}} * k_{\mathrm{v},V,\mathrm{W}}^{\mathrm{v},V,\mathrm{P}} \tag{3}$$

where the $k_{\mathrm{v},V,\mathrm{W}}^{\mathrm{v},V,\mathrm{P}}$ factor is determined experimentally from $R_{\mathrm{v},V,\mathrm{P}}$ and $R_{\mathrm{v},V,\mathrm{W}}$. Note that in E5 the total volume of aqueous solution or microparticle suspension in each vial was 20 mL. Attenuation by microparticles in the vials was clearly observed, with

$k_{\mathrm{v},20,\mathrm{W}}^{\mathrm{v},20,\mathrm{P}} = 0.9755(39)$ for the CRC-15R calibrator

and

$k_{\mathrm{v,20,W}}^{\mathrm{v,20,P}} = 0.9743(35)$ for the CRC-55tR calibrator

where the stated uncertainties are calculated by combining the standard deviation on repeat measurements of $R_{\mathrm{v},V,\mathrm{P}}$ and $R_{\mathrm{v},V,\mathrm{W}}$ in quadrature. So, the presence of $CaCO_3$ microparticles in the dose vials leads to a ≈ 2.5 % reduction in the response in the two Capintec calibrators. In the VIC, the reduction in response was less, giving $k_{\mathrm{v,20,W}}^{\mathrm{v,20,P}} = 0.9901(7)$.

Finally, when a vial was shaken (suspending the microparticles) and measured repeatedly while the particles re-settled to the bottom of the vial, the instrument (Capintec or VIC) response change was smaller than the standard deviation on repeated readings (less than about 0.3 %). VIC Monte Carlo simulations for $CaCO_3$ mixed uniformly with the water or settled into the lower 24 % of the vial (as evident for the syringe shown in Figure 1) gave results for $k_{\mathrm{v,20,W}}^{\mathrm{v,20,P}}$ of 0.9953(20) and 0.9952(20), respectively, which are comparable to the experimental value of $k_{\mathrm{v,20,W}}^{\mathrm{v,20,P}}$ = 0.9901(7) and corroborate the lack of difference in IC response observed during particle settling.

3.3. Measuring suspension of labeled microparticles in syringes (Experiment 6)

In E6 the goal was to establish dose calibrator settings for the syringe geometry (Table 5) as had been done for the dose vials.

The attenuation by the particles is described by $k_{\mathrm{s},V,\mathrm{W}}^{\mathrm{s},V,\mathrm{P}}$, which is specific to the 20 mL syringe geometry, therefore the response is calculated as:

$$R_{\mathrm{s},v,\mathrm{P}} = R_{\mathrm{s},v,\mathrm{W}} * k_{\mathrm{s},v,\mathrm{W}}^{\mathrm{s},v,\mathrm{P}} \quad (4)$$

In the syringe geometry, attenuation by the microparticles affects response in the Capintec chambers by ≈ 1 % (Table 6).

Measurements were also carried out on the VIC using the custom-built Capintec dipper for the syringes; by coincidence, the height of the radioactive material in the VIC is approximately the same for a syringe in this dipper and a vial in its dipper. For 12 mL of water in the 20 mL syringe, K_{VIC} = 14.25(5) pA/MBq and attenuation by microparticles led to $k_{\mathrm{s},12,\mathrm{W}}^{\mathrm{s},12,\mathrm{P}} = 0.993(5)$.

4. Conclusions

Calibration factors (or dials settings) relating ionization chamber responses for $^{224}RaCl_2$ solution and ^{224}Ra adsorbed onto $CaCO_3$ microparticles in different measurement geometries were determined and presented. In the Capintec radionuclide calibrators considered here, ampoules and vials containing $^{224}RaCl_2$ solution give a response consistent to < 1 %. For ^{224}Ra adsorbed onto $CaCO_3$ microparticles at a concentration of 250 mg/mL, photon attenuation results in a reduction in response varying from ≈ 1 % to ≈ 2.5 % in the geometries considered here. The *in situ* procedure yields high labeling efficiency (> 99 %) with no observable desorption.

A drug product based on ^{224}Ra adsorbed onto $CaCO_3$ microparticles has shown promise in preclinical studies for the treatment of micrometastatic diseases in body cavities (Westrøm et al., 2018, 2018b). To enable precise dose-response relationships, NIST has developed calibration

settings for a set of commercially available and clinically relevant reentrant ICs for ^{224}Ra in 5 mL flame-sealed ampoules, 20 mL dose vials, and 20 mL syringes.

The results of the measurements reported herein should be considered valid only for the containers and solution compositions described and variations of these will impact ionization chamber responses. Moreover, users should verify the validity of the dial settings on their own systems and always follow manufacturer instructions when assaying drug products. Still, the trends in and magnitude of attenuation effects revealed here should inform future calibrations and provide a benchmark for clinical assays of ^{224}Ra-based radiopharmaceuticals.

Declaration of competing interest

This work was funded in part by Oncoinvent AS, Norway. EN is employed by and owns stock in Oncoinvent AS, Norway. GEH is employed by and behold stock options in Oncoinvent AS, Norway. EN was supported by the Industrial PhD project n.259820/030 of the Norwegian National Research Council. No other potential conflicts of interest relevant to this article exist.

Acknowledgments

EN was supported by the Industrial PhD project n.259820/030 of the Norwegian National Research Council.

References

Bé, M.-M., Chisté, V., Dulieu, C., Browne, E., Chechev, V., Kuzmenko, N., Helmer, R.,

Nichols, A., Schönfeld, E., Dersch, R., 2004. Table of Radionuclides (Vol. 2 – A = 151 to 242). Monographie BIPM-5.

Bergeron DE, Cessna JT, 2018. An update on ‘dose calibrator’ settings for nuclides used in nuclear medicine. Nucl. Med. Commun. 39, 500-504.

Calhoun, J.M., Golas, DB, Harris SG, 1987. Effects of varying geometry on dose calibrator response-Co-57 and Tc-99 m. J. Nucl. Med.28, 1478–1483.

Eckert & Ziegler. Eckert & Ziegler stoppt klinische Entwicklung von SpondylAT®; 2006. Accessed Nov 2019: http://www.ezag.com/de/startseite/presse/pressemeldungen/detail/?tx_ttnews%5Btt_news%5D=425&cHash=e69ca5ac3dcd82b7ed0efd648b88c474.

Fitzgerald R., 2010. An automated ionization chamber for secondary radioactivity standards. Appl Radiat Isot. 37, 403-408.

Juzeniene A, Bernoulli J, Suominen M, Halleen J, Larsen RH, 2018. Antitumor Activity of Novel Bone-seeking, α-emitting ^{224}Ra-solution in a Breast Cancer Skeletal Metastases Model. Anticancer research Apr 1, 38(4):1947-55.

Koch W., 1978. Indication for ^{224}Ra-therapy in ankylosing spondylitis (Morbus Struempell-Bechterew-Marie). Biological Effects of ^{224}Ra. Springer, Dordrecht.pp.21-29.

Kluetz PG, Pierce W, Maher VE, et al., 2014. Radium Ra 223 dichloride injection: US Food and Drug Administration drug approval summary. Clin Cancer Res. 20(1), 9-14.

Kommission Pharmakotherapie, 2001. Stellungnahme der Deutschen Gesellschaft für Rheumatologie zur Therapie der ankylosierenden Spondylitis (AS) mit Radiumchlorid (^{224}SpondylAT®). Z Rheumatol 60, 84-87.

Elisa Napoli, Jeffrey T. Cessna, Ryan Fitzgerald, Leticia Pibida, Ronald Collé, Lizbeth Laureano-Pérez, Brian E. Zimmerman, Denis E. Bergeron, 2020. Primary standardization of ^{224}Ra activity by liquid scintillation counting. Appl Radiat Isot.155, 108933.

Pappenheim A, Plesch J., 1912. Einige Ergebnisse uber experimentelle und histologische Untersuchungen zur Wirkung des Thorium X auf den tierischen Organismus. Berl. klin. Wchnschr 49, 1342.

Rogers DWO, Kawrakow I, Seuntjensv JP, Walters BRB, Mainegra-Hing E, 2010. NRC User Codes for EGSnrc, NRC Report PIRS-702(RevB).

Rosenshein NB, Leichner PK, Vogelsang G., 1979. Radiocolloids in the treatment of ovarian cancer. Obstet Gynecol Surv 34(9), 708-720

Sartor O, Hoskin P, Bruland ØS, 2013, Targeted radio-nuclide therapy of skeletal metastases. *Cancer Treat Rev*. 39(1), 18-26.

Sibbens G, Altzitzoglou, T., 2007. Preparation of radioactive sources for radionuclide metrology. Metrologia 44, S71-78.

Townson R, Tessier F, Galea R, 2018. EGSnrc calculation of activity calibration factors for the Vinten Ionization Chamber. Appl Radiat Isot. 134, 100-104.

US National Research Council, 1988. Health risks of radon and other internally deposited alpha-emitters: BEIR IV. National Academies Press.

Wick RR, and Gössner W, 1993. History and current uses of 224Ra in ankylosing spondylitis and other diseases. Environment international. 19.5, 467-473.

Westrøm, S., Malenge, M., Jorstad, I.S., Napoli, E., Bruland, Ø.S., Bønsdorff, T.B., Larsen, R.H., 2018a. Ra-224 labeling of calcium carbonate microparticles for internal α-therapy: Preparation, stability, and biodistribution in mice. J. Label. Compd. Radiopharm., 61, 472-86.

Westrøm, S., Bønsdorff, T. B., Bruland, Ø. S., & Larsen, R. H., 2018b. Therapeutic Effect of α-Emitting ^{224}Ra-Labeled Calcium Carbonate Microparticles in Mice with Intraperitoneal Ovarian Cancer. Transl. Oncol., *11*(2), 259-267.

Zimmerman, B.E., Cessna, J.T., 2000. Experimental determinations of commercial ‘dose calibrator’ settings for nuclides used in nuclear medicine. Appl. Radiat. Isot. 52, 615-619.

Zimmerman BE, Kubicek GJ, Cessna, JT, Plascjak PS, Eckelman WC, 2001. Radioassays and experimental evaluation of dose calibrator settings for F-18. Appl Radiat Isot.54, 113–122.

Zimmerman BE, Bergeron DE, Cessna, JT, Fitzgerald R, Pibida, L, 2015. Revision of the NIST standard for ^{223}Ra: New measurements and review of 2008 data. J. Res. NIST, 120, 37-57.

source	IC	*DS*	u_A / %
A2	CRC-15R	739(4)	0.46
	CRC-55tR	737(4)	0.47
V1 (20 mL)	CRC-15R	737(4)	0.44
	CRC-55tR	735(4)	0.45
	CRC-25PET	741(5)	0.59
V7 (2 mL)	CRC-15R	744(4)	0.46
	CRC-55tR	740(4)	0.46
	CRC-25PET	747(5)	0.54

Table 1 Dial settings (*DS*) determined in E4. Combined standard uncertainties on the *DS*s are shown in parentheses following the setting. These uncertainties are translated to the relative uncertainty on the activity reading at that setting (u_A / %).

Uncertainty Component	u_i / %
Source activity; estimated from the uncertainty on the standard activity concentration and the weighing uncertainty	0.28
Decay correction; propagation of the uncertainty (0.06 %) on the DDEP half-life for ^{224}Ra	0.001
Reproducibility; estimated source-to-source variance, propagated from the standard deviation on the IC response to the three vials containing 20 mL of solution	0.22
Fit error; estimated from the standard error of the fit for the calibration curve data, fully encompassing uncertainty due to measurement repeatability	0.44
Combined standard uncertainty: $u_c = (\Sigma u_i^2)^{1/2}$	0.56
u_c expressed in DS units	4
u_A; impact of u_c on the activity reading / %	0.46

Table 2 Example dial setting uncertainty budget taken from the E4 DS determination for a dose vial containing 2 mL of $^{224}RaCl_2$ in HCl.

Capintec chambers	CRC-15R		CRC-55tR	
	k	u_c	k	u_c
$k_{\mathrm{a,5,A}}^{\mathrm{v,20,A}}$	0.9978	0.0015	0.9982	0.0022
$k_{\mathrm{v,20,A}}^{\mathrm{v,20,W}}$	1.0022	0.0019	1.0007	0.0021
$k_{\mathrm{v,20,W}}^{\mathrm{v,2,W}}$	1.0030	0.0027	1.0042	0.0015
$k_{\mathrm{v,20,A}}^{\mathrm{v,2,A}}$	1.0055	0.0022	1.0042	0.0011

Table 3 Correction factors calculated from chamber responses (see equations 1 & 2 for an explanation of $k_{\mathrm{a,5,A}}^{\mathrm{v},V,\mathrm{A}}$ and $k_{\mathrm{v},V,\mathrm{A}}^{\mathrm{v},V,\mathrm{W}}$). Volume corrections relating the response measured at 2 mL to the expected response at 20 mL are expressed as $k_{\mathrm{v,20,W}}^{\mathrm{v,2,W}}$ or $k_{\mathrm{v,20,A}}^{\mathrm{v,2,A}}$. The uncertainties on the factors are estimated by combining the standard deviation of the mean on repeated measurements of each source (typically ≈ 0.03 %) with the standard deviation on the relative response determined for each geometry, including source-to-source variance (≈ 0.1 % to 0.2 %).

VIC	k	u_c
$\boldsymbol{k}_{\mathbf{a,5,A}}^{\mathbf{v,20,A}}$	0.9815	0.0063
$\boldsymbol{k}_{\mathbf{v,20,A}}^{\mathbf{v,20,W}}$	1.0017	0.0111
$\boldsymbol{k}_{\mathbf{v,20,W}}^{\mathbf{v,2,W}}$	1.0233	0.0105
$\boldsymbol{k}_{\mathbf{v,20,A}}^{\mathbf{v,2,A}}$	1.0219	0.0029

Table 4 Correction factors calculated from VIC responses. See equations 1 & 2 for an explanation of $k_{\mathrm{a,5,A}}^{\mathrm{v},V,\mathrm{A}}$ and $k_{\mathrm{v},V,\mathrm{A}}^{\mathrm{v},V,\mathrm{W}}$. Volume corrections relating the response measured at 2 mL to the expected response at 20 mL are expressed as $k_{\mathrm{v,20,W}}^{\mathrm{v,2,W}}$ or $k_{\mathrm{v,20,A}}^{\mathrm{v,2,A}}$. The uncertainties on the factors are estimated by combining the standard deviation of the mean on repeat measurements of each source (≈ 0.1 %) with the standard deviation on the relative response determined for each geometry, including source-to-source variance (≈ 0.2 % to 1 %).

	CRC-15R	CRC-35R	CRC-55tR	CRC-25PET	CRC-55tPET
Ampoule	739(4)	747(9)	736(4)	739(5)	731(4)
Syringe	753(5)	762(9)	752(4)	755(5)	747(4)
Syringe P	745(4)	754(9)	745(4)	747(6)	741(5)

Table 5 Dial settings determined in E6 for ampoules and syringes containing ^{224}Ra in equilibrium with its progeny with and without labeled $CaCO_3$ microparticles (Syringe and Syringe P). Combined standard uncertainties are given in parentheses following the dial settings.

	CRC-15R	CRC-35R	CRC-55tR	CRC-25PET	CRC-55tPET
$k_{s,12,W}^{s,12,P}$	0.9915(12)	0.9907(32)	0.9913(9)	0.9908(30)	0.9925(20)

Table 6 Correction factors calculated from chamber responses and Equation 4. The uncertainties on the factors are estimated by combining the standard deviation of the mean on repeat measurements of each source (0.03 % to 0.32 %) with the standard deviation on the relative response determined for each geometry (0.04 % to 0.29 %).

Figure 1 Syringes with and without $CaCO_3$ microparticles prepared and measured in E6. The total volume of solution is the same in both syringes. When agitated, the sedimented particles (visible in the syringe on the left) suspend into the water, but the IC response is not measurably affected.

Figure 2 The decay-corrected (using only the ^{224}Ra half-life) activity calculated from the response of an ionization chamber increases until secular equilibrium is achieved. The VIC and CRC-55tR readings shown here were acquired with an equilibrating ampoule in E4. The uncertainty bars are the standard deviation of repeat measurements. All *DS*s and correction factors reported herein are calculated from data acquired at secular equilibrium.

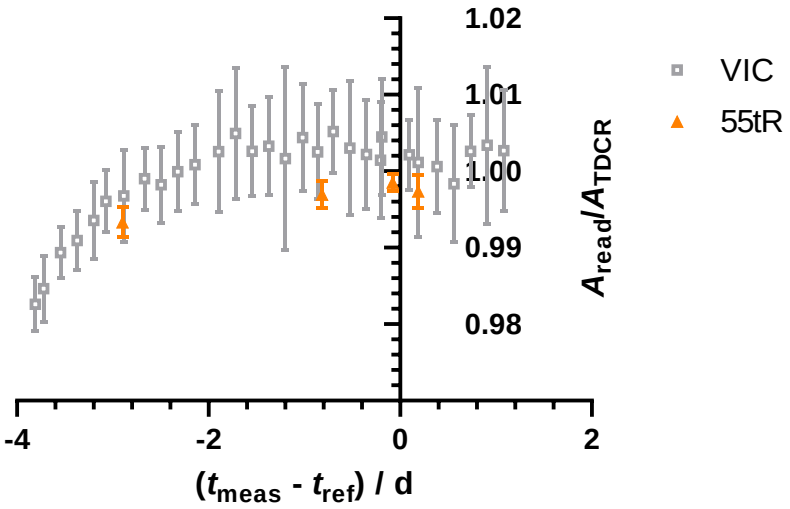

Figure 3 Response of the Capintec CRC-15R and CRC-55tR chambers, normalized by the TDCR-determined activities for the series of vials (E4-V1 to E4-V7) containing 2 mL to 20 mL of ^{224}Ra in 1 mol/L HCl. All vials were measured at *DS* = 742 on the CRC-15R and *DS* = 740 on the CRC-55tR; vial-specific *DS*s for these chambers can be found in Table 1. Uncertainty bars represent the standard deviation on 10 repeat measurements.

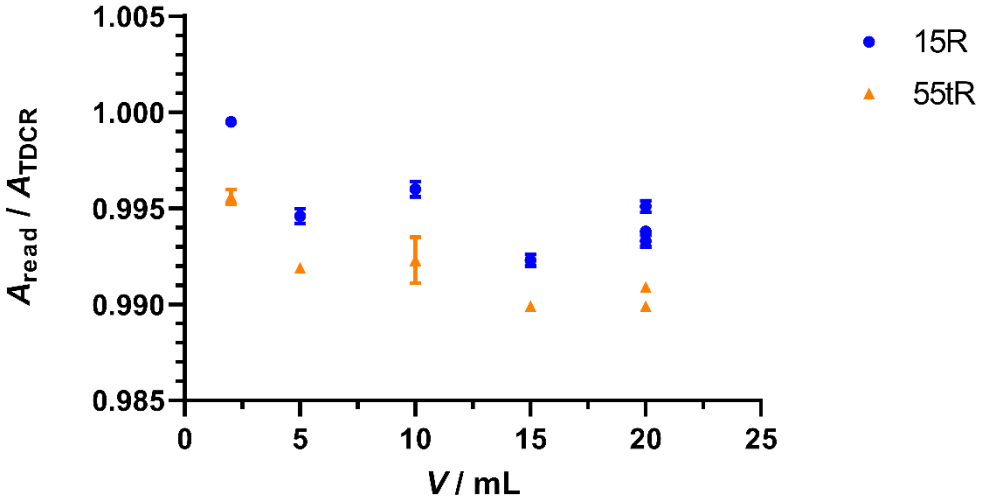

Figure 4 Calibration coefficients for the VIC (K_{VIC}) determined experimentally (blue) and by Monte Carlo calculation (red) for the series of vials (E4-V1 to E4-V7) containing 2 mL to 20 mL of ^{224}Ra in 1 mol/L HCl. The uncertainty bars in the experimental series represent estimated counting uncertainties (typical standard deviation of the mean for 200 current measurements (typically ≈ 0.1 %) combined with the standard deviation on measurements on multiple (N = 2 to 3) occasions (typically ≈ 0.1 % to 0.2 %)). The uncertainty bars on the Monte Carlo points are statistical, calculated from the standard deviation on > 2 million histories per point.

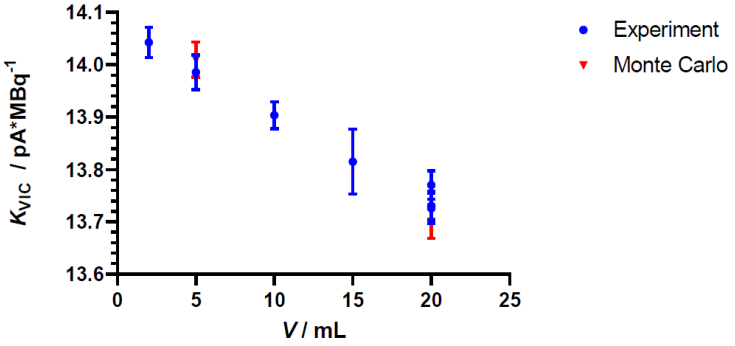

Figure 5 Labeling efficiency study. The ionization chamber response for each vial (L*X*, where *X* = 1 to 3) normalized by the contemporaneous response for L0. The closed symbols correspond to vials with supernatant; open symbols are vials from which supernatant has been removed. The uncertainty bars correspond to the standard deviation on 10 repeat measurements.